

# Mechanical property relationships in glass-filled polyoxymethylene

S. HASHEMI

*University of North London, School of Polymer Technology, Holloway Road, London N7 8DB, UK*

M. T. GILBRIDE, J. HODGKINSON

*Imperial College of Science, Technology and Medicine, Composite Centre, Exhibition Road, London SW5 3RB, UK*

The dependence of the mechanical properties such as strength, modulus and fracture toughness on the volume fraction of the reinforcing glass fibres and glass beads in polyoxymethylene (POM) matrix was studied. The majority of the measured quantities in tension or flexure tests, seemed to be linear functions of either the volume fraction of the glass fibres or the glass beads. The relationship between some individual mechanical properties seemed to be linear as well. Consequently, many of the mechanical properties of these POM composites (POM/GF and POM/GB) could be estimated from one measured property using the relationships presented. Also, the same property measured for the two composite systems was found to be linearly related. Consequently, the mechanical properties of one composite system, (i.e. POM/GB) could be used to determine that of the other system (i.e. POM/GF) at the same filler concentration.

## 1. Introduction

Glass bead-filled and short glass fibre-filled thermoplastics are being used in a wide variety of industrial applications. While properties such as dimensional stability or increased modulus are the usual motivation for exploiting glass bead-filled composites, increase in tensile strength, modulus or fracture toughness are the usual motivation for exploiting short glass fibre-filled composites. In the case of glass bead-filled systems, poor adhesion between bead and the matrix is a primary cause of low strength, especially at high bead volume fractions. In addition, injection moulding of thermoplastics and their composites often involves circumstances leading to weldlines in the injection moulded parts which are the potential source of mechanical weakness.

In the present study, deformation and fracture behaviour of two glass polyoxymethylene filled (POM) systems are studied, namely glass bead-filled POM (POM/GB system) and short glass fibre-filled POM (POM/GF system). For each composite system filler concentration varied between 0 and 19% by volume, thus enabling us to compare the mechanical properties of the two systems as a function of filler concentration and to obtain relationships correlating properties of the two systems.

## 2. Materials

### 2.1. Matrix

The polymer matrix for all the composites investigated in the present study is a copolymer of poly(oxy-

methylene) produced by Hoechst under the trade name Hostaform C 9021. The copolymer is made from trioxane with small amounts of comonomers. It has a density of  $1.41 \text{ g cm}^{-3}$ , the melt flow index  $9.5 \text{ g/10 min}$  and the crystalline melting point in the range of  $164\text{--}167^\circ\text{C}$ . Some basic mechanical properties of the matrix polymer is given in Table 1 [1].

### 2.2. Composites

Six grades of filled polyoxymethylene material were supplied by Hoechst UK as natural colour granules. The filled materials contained 10–30% by weight glass fibres or glass beads as listed in Table II. Volume fraction of the filler,  $\phi_{\text{filler}}$ , in each composite was calculated from the following equation using the respective densities of the constituents.

$$\phi_{\text{filler}} = \frac{\rho_{\text{composite}} w_{\text{filler}}}{\rho_{\text{filler}}} \quad (1a)$$

where  $\rho_{\text{composite}}$  is the density of the composite,  $\rho_{\text{filler}}$  is the density of the filler and  $w_{\text{filler}}$  is the weight fraction of the filler in the composite. The densities of the composites were obtained from the manufacturer, and the density of glass was taken as  $2.54 \text{ g cm}^{-3}$ .

### 3. Mouldings

Two types of specimens, as shown in Fig. 1, were injection moulded for each material;

TABLE I Matrix properties

Tensile yield strength (MPa)	56.87
Flexural strength (MPa)	118.7
Flexural modulus (GPa)	2.27
Fracture toughness (MPa m <sup>1/2</sup> )	4.27

TABLE II Composite materials

Grade	Description	$\Phi_{\text{filler}}$ (%)	$L_{\text{FIBRE}}$ ( $\mu\text{m}$ )
C9021 GV 1/10	10 wt % glass fibres	6	250
C9021 GV 1/20	20 wt % glass fibres	12	258
C9021 GV 1/30	30 wt % glass fibres	19	242
C9021 GV 3/10	10 wt % glass beads	6	
C9021 GV 3/20	20 wt % glass beads	12	
C9021 GV 3/30	30 wt % glass beads	19	

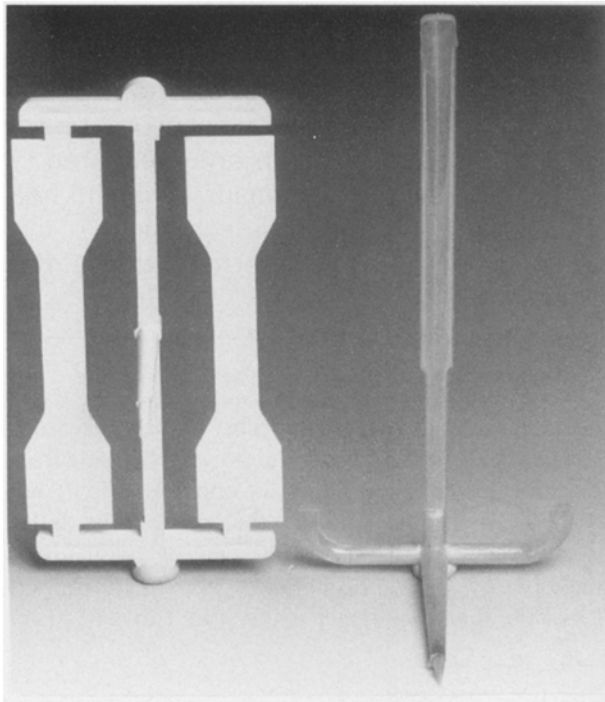


Figure 1 Moulded specimens.

### 3.1. Tensile bars

Dumbbell-shaped tensile specimens of dimensions  $1.7 \times 12.5 \times 125$  mm were produced on a Negri Bossi NB60. The mould used consisted of two cavities, a single feed and a double feed cavity, as shown in Fig. 1. In the latter, a weldline was formed by head-on collision of two opposing melt fronts.

### 3.2. Flexural bars

Flexural specimens were produced on a Szekely Hydrojet injection moulding machine using an edge-gated rectangular cavity of dimensions  $4 \times 10 \times 120$  mm, as shown in Fig. 1.

Table III summarises the range of processing conditions used for producing glass fibre and glass bead filled mouldings.

TABLE III Processing conditions

Glass fibre-filled materials (POM/GF):	
Melt temperature ( $^{\circ}\text{C}$ )	195–200
Mould temperature ( $^{\circ}\text{C}$ )	80
Injection pressure (psi)	655.5–724.5 kPa
Injection time (s)	5–10
Cooling time (s)	10–20
Glass bead-filled materials (POM/GB):	
Melt temperature ( $^{\circ}\text{C}$ )	195–200
Mould temperature ( $^{\circ}\text{C}$ )	80
Injection pressure (psi)	414–552 kPa
Injection time (s)	5–10
Cooling time (s)	15–20

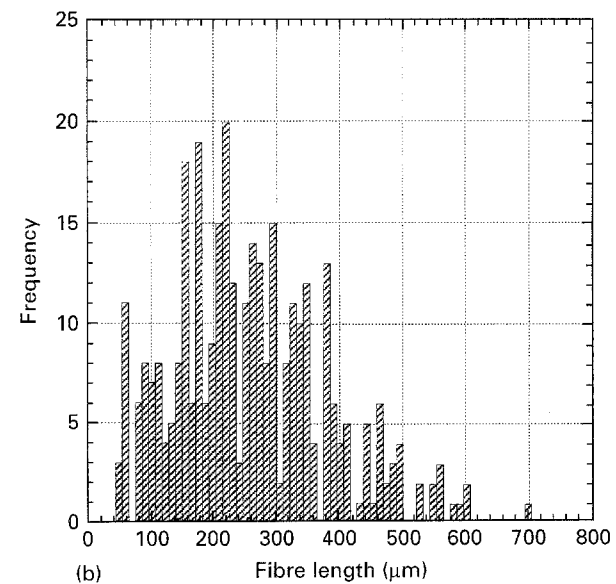
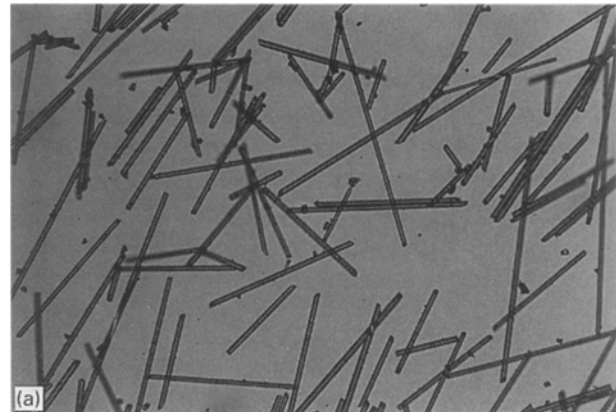


Figure 2 (a) Optical micrograph of the fibres in POM/GF with  $\Phi_{\text{FIBRE}} = 12\%$ . (b) Fibre length frequency for POM/GF with  $\Phi_{\text{FIBRE}} = 12\%$ .

## 4. Fibre length distribution

The measurement of the length of the fibre in the fibre reinforced grades was carried out by burning off the organic polymer matrix in a muffle furnace at a temperature of  $600^{\circ}\text{C}$ . The char remaining in the muffle was then viewed under an optical microscope and a series of photographs (see the example shown in Fig. 2(a)) were taken from which some 500 fibre lengths were counted. The frequency distribution of

fibre lengths was then plotted (see the example shown in Fig. 2(b)) and the mean fibre length,  $L_{\text{FIBRE}}$ , for each grade was determined (see Table II). As can be seen  $L_{\text{FIBRE}}$  does not vary significantly from one grade of material to another. The mean diameter of the fibres,  $d_{\text{FIBRE}}$ , was  $8 \mu\text{m}$  compared to that of glass beads which was  $30 \mu\text{m}$ .

The critical length of the reinforcing fibres,  $L_{c,\text{FIBRE}}$ , was estimated from the following equation

$$L_{c,\text{FIBRE}} = \frac{d_{\text{FIBRE}} \sigma_{\text{FIBRE}}}{2\tau_{\text{POM}}} \quad (1.b)$$

Taking the shear strength of the POM matrix as  $\tau_{\text{POM}} = \sigma_{\text{POM}} 3^{-1/2} = 33 \text{ MPa}$  (in accordance with the von Mises yield criterion) and tensile strength of the fibre ( $\sigma_{\text{FIBRE}}$ ) as  $2.47 \text{ GPa}$ , we obtained a critical fibre length value of  $300 \mu\text{m}$ . The actual length of the fibres is thus near or somewhat less than the critical length.

## 5. Mechanical testing

### 5.1. Tensile tests

Tensile tests were performed on dumbbell specimens with and without weldlines at room temperature in an Instron testing machine at a crosshead displacement rate of  $5 \text{ mm min}^{-1}$ . Nominal tensile yield stress for each material was determined using the maximum load on the load-displacement diagram.

### 5.2. Flexural tests

Three-point flexural tests were performed on the flexural bars of dimensions  $B = 10 \text{ mm}$  and  $D = 4 \text{ mm}$  (see Fig. 3(a)). Tests were performed at room temperature in an Instron testing machine. The span length for all the tests was  $64 \text{ mm}$ , and the cross-head speed was  $5 \text{ mm min}^{-1}$ . Load-displacement trace for each specimen was recorded and was used to calculate flexural modulus and strength via the following equations

$$\sigma_{\text{flex}} = \frac{3P_{\text{max}}S}{2BD^2}$$

$$E_{\text{flex}} = \frac{1}{4B} \left( \frac{P}{\delta} \right) \left( \frac{S}{D} \right)^3 \quad (2)$$

where  $P_{\text{max}}$  is the maximum load,  $(P/\delta)$  is the initial slope,  $S$  is span length and  $B$  and  $D$  are specimen thickness and depth, respectively.

### 5.3. Impact tests

Unnotched impact strength was measured using flexural bars of dimensions  $B = 4 \text{ mm}$  and  $D = 10 \text{ mm}$  (see Fig. 3(b)). Specimens were impacted at room temperature at a pendulum speed of  $3 \text{ m s}^{-1}$  with span to depth ratio set at 4:1.

### 5.4. Fracture toughness tests

Fracture toughness tests were performed using single-edge notched bend specimens (SENB) of dimensions

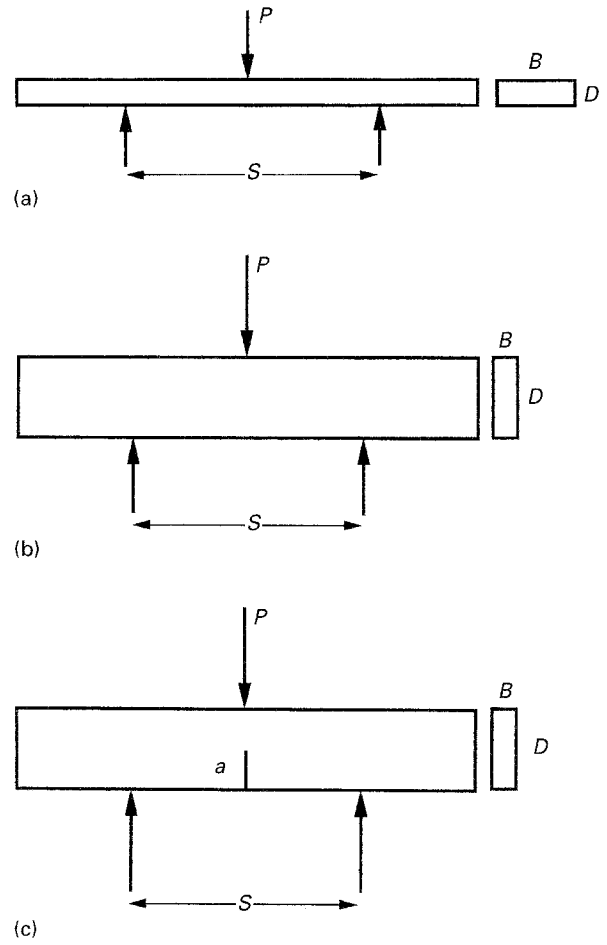


Figure 3 Specimen geometries; (a) flexural modulus, (b) Charpy impact and (c) single-edge notched bend (SENB).

$B = 4 \text{ mm}$ ,  $D = 10 \text{ mm}$  (see Fig. 3(c)). Single-edge notch of various lengths was inserted using a razor blade; notch depth,  $a$ , varied from  $0.1D$  to  $0.6D$ . All tests were performed at room temperature in an Instron testing machine at a crosshead displacement rate of  $5 \text{ mm min}^{-1}$ . Span width,  $S$ , was set at  $40 \text{ mm}$  thus giving an  $S/D$  ratio of 4:1.

Fracture toughness,  $K_{Ic}$ , was calculated for each material using the relationship [2]

$$K_{Ic} = \sigma_c Y a^{1/2} \quad (3)$$

where  $\sigma_c$  is the fracture stress and  $Y$  is a geometrical factor whose value for SENB specimens can be calculated from the following functions [2]

$$Y = 1.93 - 3.07x + 14.53x^2 - 25.11x^3 + 25.8x^4 \quad (4)$$

where  $x = a/D$  ratio.

## 6. Results and discussion

### 6.1. Tensile properties

Tensile load-displacement diagrams for the POM matrix and its glass bead-filled composites exhibited a clear yield point whereas those of glass fibre composite materials were typically brittle, i.e. fracturing at the maximum load. During the yielding of the POM/GB specimens, some degree of stress whitening took place which became more severe as glass bead concentration was increased. This stress whitening

phenomenon resulted from vacuole formation around the glass beads as they separated from the matrix under load.

Several empirical relationships have been proposed for predicting the tensile strength of the glass bead filled systems. The most widely used of these are the Nicolias and Narkis [3] and Piggott and Leidner [4] equations. The former suggests that tensile strength of the glass bead system,  $\sigma_{\text{MATRIX/GB}}$ , decreases non-linearly with increasing volume fraction of glass beads,  $\phi_{\text{BEAD}}$ , whereas the latter suggests that it decreases linearly with  $\phi_{\text{BEAD}}$  according to the following relationship

$$\sigma_{\text{MATRIX/BEAD}} = \lambda\sigma_{\text{MATRIX}} - \alpha\phi_{\text{BEAD}} \quad (5)$$

where  $\sigma_{\text{MATRIX}}$  is the tensile yield strength of the matrix,  $\lambda$  is a stress concentration factor and  $\alpha$  is a constant whose value depends on the particle–resin adhesion. Fig. 4 shows that the variation of tensile yield strength of the POM/GB composites ( $\sigma_{\text{POM/GB}}$ ) with the volume fraction of the glass beads,  $\phi_{\text{BEAD}}$ , is linear for the range of  $\phi_{\text{BEAD}}$  values used in this study. A good fit was obtained by using the theory of Piggott and Leidner as embodied in the following equation

$$\sigma_{\text{POM/GB}} = \sigma_{\text{POM}}(1 - 1.72\phi_{\text{BEAD}}) \quad (6)$$

giving  $\lambda$  and  $\alpha$  values of 1 and 97.77, respectively. The negative slope in Equation 6 indicates that the presence of glass bead has a weakening effect rather than a strengthening one. This is because as glass beads debond from the matrix material due to poor adhesion, the volume fraction of the composite carrying the load is reduced. The higher the glass bead concentration, the lower the volume fraction of the composite carrying the load.

As for the POM/GF system, since the actual length of the fibres is near (or somewhat less than) the critical length, the tensile strength of the fibre does not itself contribute to the strength of the composite; although the presence of fibres does nonetheless make some contribution. Tensile strength of the injection moulded short fibre composites,  $\sigma_{\text{POM/FIBRE}}$ , for the case in which  $L_{\text{FIBRE}} \leq L_{c, \text{FIBRE}}$  is generally described

by the Kelly and Tyson [5] relationship

$$\sigma_{\text{POM/GF}} = \eta_0 \frac{\sigma_{\text{FIBRE}} L_{\text{FIBRE}}}{2L_c} \phi_{\text{FIBRE}} + (1 - \phi_{\text{FIBRE}}) \sigma_{\text{POM}} \quad (7)$$

where  $\sigma_{\text{FIBRE}}$  is the tensile strength of the fibres,  $\phi_{\text{FIBRE}}$  is the volume fraction of the fibres and  $\eta_0$  is the fibre orientation efficiency factor. The above equation can be expressed in the following form

$$\sigma_{\text{POM/GF}} = \sigma_{\text{POM}}(1 + \beta\phi_{\text{FIBRE}}) \quad (8)$$

where  $\beta$  is given by

$$\beta = \frac{\eta_0 \sigma_{\text{FIBRE}} L_{\text{FIBRE}}}{2\sigma_{\text{POM}} L_c} - 1 \quad (9)$$

Assuming that for a given composite system,  $\beta$  is constant, then the relationship between  $\sigma_{\text{POM/GF}}$  and  $\phi_{\text{FIBRE}}$  is expected to be linear as found here (see Fig. 4). The best regression line fitted through the data gave

$$\sigma_{\text{POM/GF}} = \sigma_{\text{POM}}(1 + 4.62\phi_{\text{FIBRE}}) \quad (10)$$

From the slope of the line and Equation 8 we estimate the orientation efficiency factor  $\eta_0$  to be 0.3, which is somewhat higher than the value of 0.2 reported for randomly oriented fibres in three dimensions [6]. This may not be unreasonable when considering that in a simple mould cavity of the type considered here, the fibre orientation is predominately along the fill direction within a shell layer at all the mould surfaces, and predominately transverse to the fill direction in the core of the moulding. Thus, fibres are more orderly oriented and not quite randomly oriented in three dimensions.

The influence of weldline on tensile strength of POM/GB and POM/GF composites can be seen from Fig. 5(a). Evidently, weldline strength of POM/GB and POM/GF systems show linear variation with respect to filler content. In the case of the POM/GB system, weldline strength decreases with increasing  $\phi_{\text{BEAD}}$  whereas in the case of POM/GF composites it increases with increasing  $\phi_{\text{FIBRE}}$ , thus exhibiting similar variations with filler content as those obtained for the weld free specimens. Accordingly, a weldline integrity parameter,  $F$ , was defined as

$$\text{Weldline integrity parameter, } F = \frac{\text{weldline strength}}{\text{weld - free strength}}$$

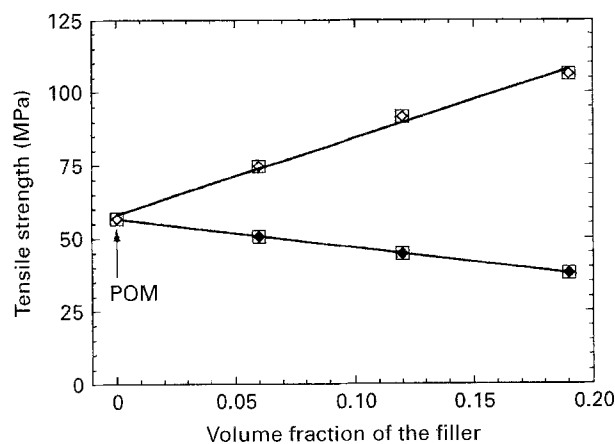


Figure 4 Tensile strength of POM/GF (□x) and POM/GB (□•) systems versus the volume fraction of the filler.

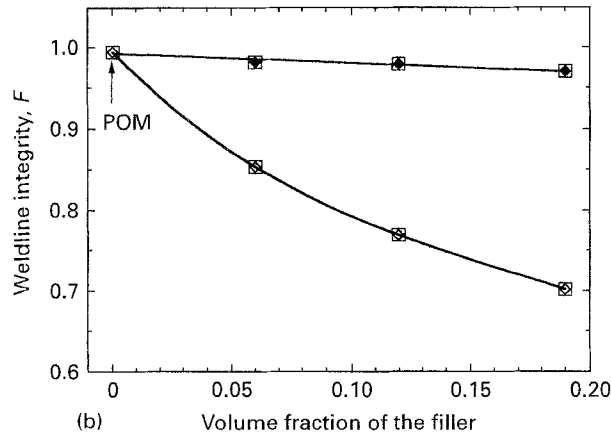
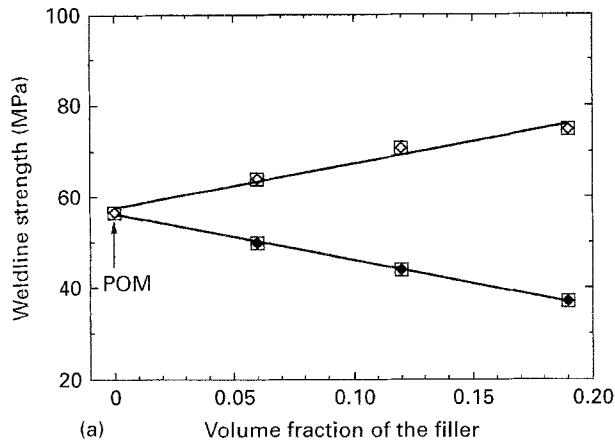


Figure 5 (a) Weldline strength of POM/GF (⊗) and POM/GB (⊙) systems versus the volume fraction of the filler. (b) Weldline integrity factor for POM/GF and POM/GB systems versus the volume fraction of the filler.

direction of the applied stress. However, results do indicate that fibres are still beneficial as reinforcing fillers, albeit to a lesser extent.

## 6.2. Flexural properties

Flexural strength of POM/GB and POM/GF composites are plotted in Fig. 6 as a function of filler content,  $\phi$ . Evidently, variation of the flexural strength for both systems is linear with respect to  $\phi$

$$\begin{aligned}\sigma_{\text{POM/GB}} &= \sigma_{\text{POM}}(1 - 1.30\phi_{\text{BEAD}}) \\ \sigma_{\text{POM/GF}} &= \sigma_{\text{POM}}(1 + 1.71\phi_{\text{FIBRE}})\end{aligned}\quad (11)$$

It is however evident from the data, that flexural strengths of POM, POM/GB and POM/GF materials are all consistently higher than their respective tensile strengths. This was partly due to the occurrence of some degree of yielding (or “plastic collapse”) during the flexure tests. Analysis of plastic bending of rectangular cross-section beams has shown that beams can carry 50% additional moment to that which is required to produce initial yielding at the edges of the beam section before a fully plastic hinge is formed. This suggests that flexural strength under the plastic collapse condition is expected to be 1.5 times that of the tensile yield strength. The strength ratios (flexural strength/tensile strength) shown in Table IV suggest

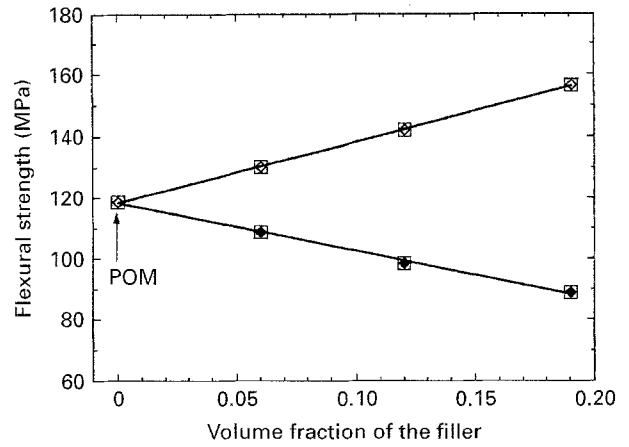


Figure 6 Flexural strength of POM/GF (⊗) and POM/GB (⊙) systems versus the volume fraction of the filler.

TABLE IV Strength ratios

Composite	Volume fraction of the filler			
	0%	6%	12%	19%
POM/GB	2.09	2.15	2.20	2.34
POM/GF	2.09	1.74	1.55	1.48

that for most composites and the POM matrix the ratio is greater than 1.5.

In the case of POM/GB system the ratio increases with increasing filler concentration, whereas the reverse is the case for POM/GF system. These strength ratios do suggest that while the plastic collapse behaviour is partly responsible for higher flexural strengths, it is not the only contributing factor. As flexural strength is dominated by the properties of the material within the surface layers and tensile strength by the properties of the material within the core section in the two mouldings, any factor influencing these properties in a different way would ultimately cause a difference in measured strengths. Factors such as: (i) differences in the outer fibre strain rate in flexure tests compared with the nominal strain rate used during the tensile tests; (ii) differences in fibre orientation distribution through the thickness of two mouldings; (iii) higher concentration of filler in the surface layers compared with that in the core section; and (iv) different degree of crystallinity at the surface layers compared with that within the core section due to differential cooling, can all be contributing factors.

Taking the flexural strength of the matrix as 118 MPa, the comparison with Equation 8 indicates that for POM/GF composites tested in flexure  $\eta_0$  is 0.50, which is higher than 0.3 obtained from tensile tests. As mentioned earlier in the flexure test, strength of the material is dominated by the properties of the material within the surface layers where fibre alignment is predominantly in the fill direction, whereas in tension tests it is dominated by the properties of the material within the core-section where fibre alignment is predominantly transverse to the fill direction. Thus, it is reasonable for flexural strengths to give a higher  $\eta_0$  value than tensile strengths.

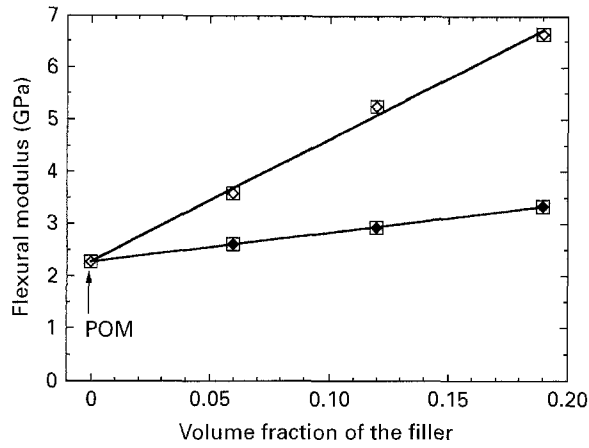


Figure 7 Flexural modulus of POM/GF (⊗) and POM/GB (■) systems versus the volume fraction of the filler.

The effect of filler content on flexural modulus is shown in Fig. 7; as expected the addition of glass fibres or glass beads improves flexural modulus of the POM matrix.

Flexural modulus of the POM/GB system is consistent with predictions for spherical filled systems as presented by Einstein [7] in which the modulus of the composite,  $E_{\text{MATRIX/GB}}$ , is expressed in terms of matrix modulus,  $E_{\text{MATRIX}}$  and the volume fraction of the spherical filler,  $\phi_{\text{BEAD}}$  as

$$E_{\text{MATRIX/GB}} = E_{\text{MATRIX}} (1 + k_E \phi_{\text{BEAD}}) \quad (12)$$

where  $k_E$  is the Einstein coefficient, given as 2.5 for spherical shape fillers. This value agrees reasonably well with the value of 2.47 obtained from the slope of the line in Fig. 7, thus indicating that for the range of  $\phi_{\text{BEAD}}$  values studied here, flexural modulus of the POM/GB system can be predicted with some degree of accuracy from the Einstein equation.

The modulus of the short glass fibre-filled materials is often expressed in terms of  $\phi_{\text{FIBRE}}$  as [6]

$$E_{\text{POM/GF}} = \eta_0 \eta_L E_{\text{FIBRE}} \phi_{\text{FIBRE}} + E_{\text{POM}} (1 - \phi_{\text{FIBRE}}) \quad (13)$$

where  $\eta_0$  as before is the fibre orientation efficiency factor and  $\eta_L$  is the fibre length efficiency factor which is defined as

$$\eta_L = 1 - \frac{\tanh x}{x} \quad \text{where} \quad x = \frac{\xi L_{\text{FIBRE}}}{2} \quad \text{and} \quad \xi = \left( \frac{8G_{\text{POM}}}{E_{\text{FIBRE}} d_{\text{FIBRE}}^2 \ln \left( \frac{2R}{d_{\text{FIBRE}}} \right)} \right)^{1/2} \quad (14)$$

where  $G_{\text{POM}}$  is the matrix shear modulus,  $2R$  is the interfibre spacing which for hexagonal packing arrangement is related to  $\phi_{\text{FIBRE}}$  by the following equation [7]

$$\phi = \frac{\pi}{2\sqrt{3}} \left( \frac{d_{\text{FIBRE}}}{2R} \right)^2 \quad (15)$$

TABLE V

	6%	12%	19%
$d_{\text{FIBRE}}/2R$	0.26	0.36	0.46
$\gamma$	$3.259 \times 10^4$	$3.742 \times 10^4$	$4.293 \times 10^4$
$\eta_L$	0.755	0.782	0.814

Note:  $\nu_{\text{POM}} = 0.3$ ,  $G_{\text{POM}} = 2.27 \text{ GPa}$ ,  $E_{\text{FIBRE}} = 76 \text{ GPa}$   
 $G_{\text{POM}} = E_{\text{POM}}/[2(1 + \nu_{\text{POM}})] = 0.87$

Analogy with Equation 8 gives

$$E_{\text{POM/GF}} = E_{\text{POM}}(1 + \gamma \phi_{\text{FIBRE}})$$

$$\text{where } \gamma = \frac{\eta_0 \eta_L E_{\text{FIBRE}}}{E_{\text{POM}}} - 1 \quad (16)$$

According to the above equations, if parameter  $\gamma$  is reasonably constant for a given composite system then the relationship between  $E_{\text{POM/GF}}$  and  $\phi_{\text{FIBRE}}$  should be reasonably linear. As shown in Fig. 7, modulus of POM/GF system as a function of  $\phi_{\text{FIBRE}}$  can be described fairly well by the following equation

$$E_{\text{POM/GF}} = E_{\text{POM}}(1 + 10.32\phi_{\text{FIBRE}}) \quad (17)$$

Using the slope of this line and the average of the values given in Table V, we estimate that the average value of  $\eta_0$  is 0.43, which compares reasonably well with the value of 0.50 obtained from flexural strength data.

The linearity of the tensile strength, flexural strength and flexural modulus with filler concentration for both composite systems led us to the notion that these quantities could be related. Several authors have studied the correlation between strength and modulus of polymers [8,9]. For example, Brown [9] showed that the parameters increase the strength also increase the modulus and that their relationship is linear. For POM/GF system, we have noted that, the increase in modulus due to the higher glass fibre content led simultaneously to the higher flexural strength. Thus, the presence of fibres is realized in strength and modulus. However, in the case of POM/GB system, increase in flexural modulus due to the higher glass bead content led to a lower flexural strength. Nevertheless, since modulus and strength values varied linearly with  $\phi$ , some degree of correlation between these quantities was expected. As can be seen from Fig. 8(a-c), one quantity can be estimated from another with a reasonable degree of accuracy, by using the following equations

$$\begin{aligned} (\sigma_{\text{POM/GF}})_{\text{flexural}} &= 98.98 + 8.64(E_{\text{POM/GF}})_{\text{flexural}} \\ (\sigma_{\text{POM/GB}})_{\text{flexural}} &= 180.46 - 27.47(E_{\text{POM/GB}})_{\text{flexural}} \\ (\sigma_{\text{POM/GF}})_{\text{weldline}} &= 35.70 + 0.37(\sigma_{\text{POM/GF}})_{\text{unweld}} \\ (\sigma_{\text{POM/GB}})_{\text{weldline}} &= -2.62 + 1.04(\sigma_{\text{POM/GB}})_{\text{unweld}} \\ (\sigma_{\text{POM/GF}})_{\text{flexural}} &= 74.01 + 0.77(\sigma_{\text{POM/GF}})_{\text{tensile}} \\ (\sigma_{\text{POM/GB}})_{\text{flexural}} &= 28.83 + 1.58(\sigma_{\text{POM/GB}})_{\text{tensile}} \end{aligned} \quad (18)$$

It must be noted that although the above correlations can be used to predict the mechanical properties of

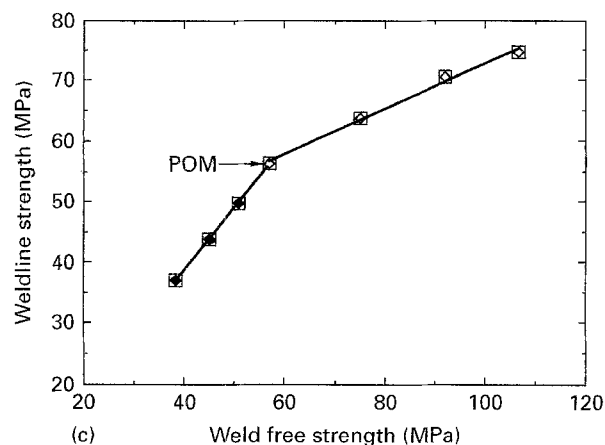
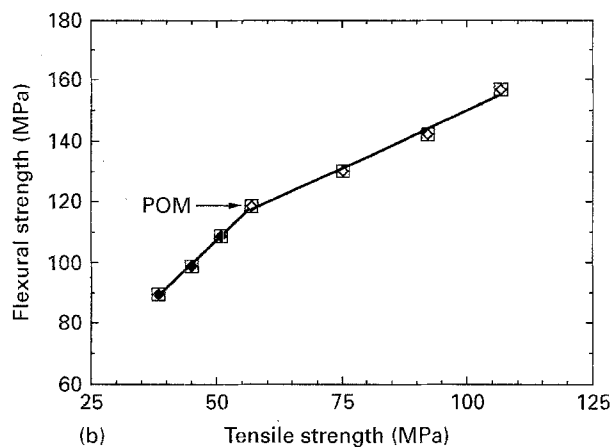
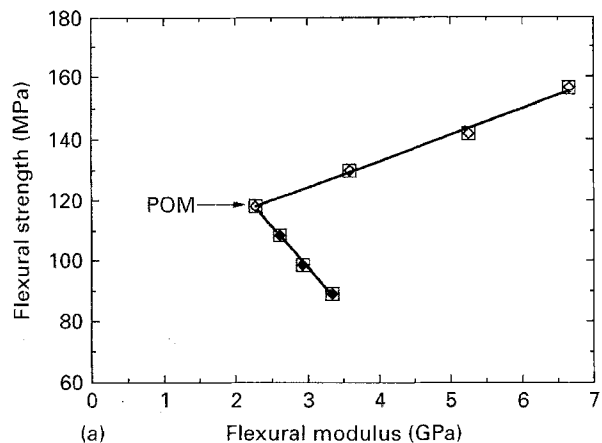


Figure 8 (a) Flexural strength versus flexural modulus for POM/GF (□) and POM/GB (■) systems. (b) Weldline strength versus weldfree strength for POM/GF and POM/GB systems. (c) Flexural strength versus tensile strength for POM/GF and POM/GB systems.

POM/GF and POM/GB composites, their quantitative use in other cases may be limited by the variation in the structural parameters and testing conditions both of which may give different results.

### 6.3. Impact tests

Fig. 9 shows the effect of filler concentration of impact strength per unit cross-section area,  $U$ , of POM/GB and POM/GF composites. Plots indicate that the addition of glass beads or glass fibres reduces the impact energy of the POM matrix considerably. The

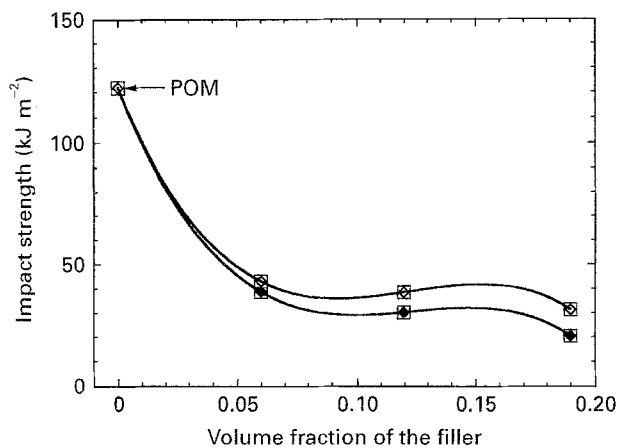


Figure 9 Impact strength versus the volume fraction of the filler for POM/GF (□) and POM/GB (■) systems.

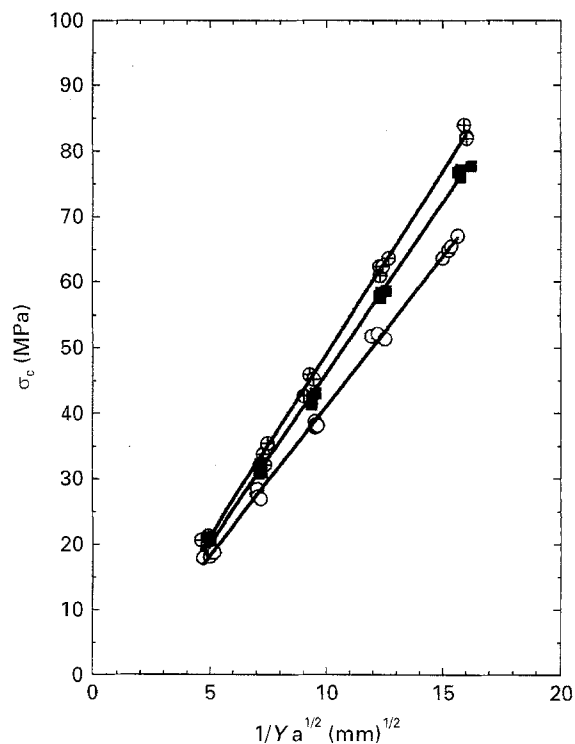


Figure 10 Fracture stress versus  $1/Ya^{1/2}$  for POM/GF system. ○ 6%; ■ 12%; ⊕ 19%.

variation of  $U$  with respect to filler content is found to be non-linear for both composite systems.

### 6.4. Fracture properties

It has been shown [1], that the fracture toughness of the POM matrix and composites in POM/GB system can be characterized by linear elastic fracture mechanics using Equation 3. Similarly, the plot of  $\sigma_c$  versus  $1/Ya^{1/2}$  (see Fig. 10) obtained in this study for each composite in POM/GF system indicated that fracture toughness is almost independent of crack length. This observation is a verification of the applicability of linear elastic fracture mechanics (LEFM) concepts to these composites.

The effect of filler concentration on fracture toughness of POM/GF and POM/GB systems is shown in

Fig. 11(a). As can be seen, whereas the addition of the glass fibres enhances the fracture toughness of the POM matrix, the addition of the glass beads reduces fracture toughness. In general the presence of glass beads could either have a toughening or a weakening effect. On the one hand since the localized stress (hence strain) is highest at the notch tip, particle debonding occurs. A notch tip damage zone is then formed which consists of a porous matrix. The modulus of this damage zone is obviously less than that of surrounding (undamaged) composite and since the notch tip stresses scale with modulus, the localized stress falls as the tip damage accumulates. This can be thought of as a strengthening mechanism. On the other hand this damage zone is weaker than the surrounding undamaged composite. Hence, a competition exists between the reduction in localized stresses (toughening effect) and the weakened matrix brought about by the creation of holes and voids around particles; the toughening of the composite depends upon which ever mechanism predominates. From the results obtained here, it appears that it is the later mechanism which controls the toughness of the POM/GB system rather than the former. As shown in Fig. 11(a), variation of  $K_c$  with  $\phi$  for POM/GF system is fairly linear, but that of POM/GB is less so. For the POM/GF system, variation of  $K_c$  with  $\phi_{\text{FIBRE}}$  can be

reasonably expressed as

$$K_{c, \text{POM/GF}} = K_{c, \text{POM}}(1 + 1.64\phi_{\text{FIBRE}}) \quad (19)$$

Using linear elastic fracture mechanics concepts, strain energy release rate,  $G_c$ , was calculated for both composite systems using the following relationship

$$G_c = \frac{K_c^2}{E} \quad (20)$$

Results obtained from the above equations are plotted in Fig. 11(b), where it can be seen that the relationship between  $G_c$  and the volume fraction of the filler is non-linear for both composite systems and decreases as glass bead or glass fibre concentrations increase.

## 7. Correlations

Thus far we have presented several relationships which enables one to either evaluate mechanical properties for a given systems as a function of filler concentration or to estimate the value of one property (e.g. flexural strength) knowing the value of another property (e.g. tensile strength) of the same system at the same volume fraction of the filler. It was found also, that when the same property for the two composite systems (i.e. POM/GF and POM/GB) at the same volume fraction of the filler was plotted against each other, the behaviour was extremely linear. These plots are presented in Fig. 12(a-d) and are fairly well described by the following equations

$$\sigma_{\text{POM/GF}} = 211.05 - 2.69\sigma_{\text{POM/GB}} \quad (\text{tensile})$$

$$\sigma_{\text{POM/GF}} = 274 - 1.31\sigma_{\text{POM/GB}} \quad (\text{flexural})$$

$$E_{\text{POM/GF}} = -7.19 + 4.17 E_{\text{POM/GB}} \quad (\text{flexural})$$

$$U_{\text{POM/GF}} = 10.66 + 0.91 U_{\text{POM/GB}} \quad (\text{impact})$$

$$K_{c, \text{POM/GF}} = 8.21 - 0.93 K_{c, \text{POM/GB}} \quad (\text{SENB})$$

$$G_{c, \text{POM/GF}} = 2.96 + 0.63 G_{c, \text{POM/GB}} \quad (\text{SENB}) \quad (21)$$

(The linear regression coefficient for the above equations was typically 0.97, except for the fracture toughness,  $K_c$  where the value was 0.90.)

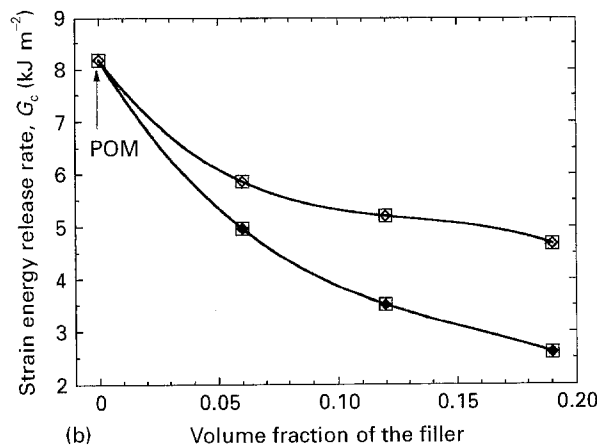
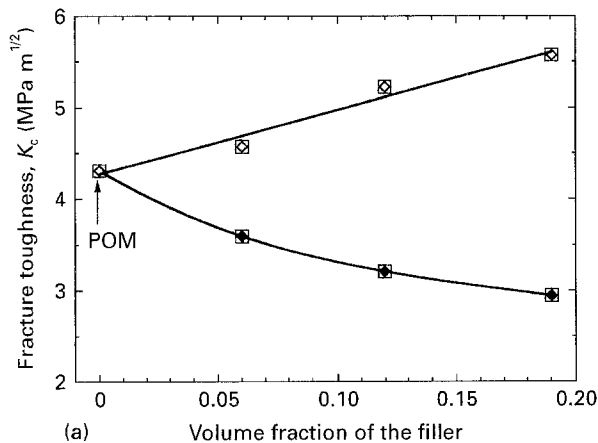


Figure 11 (a) Fracture toughness versus the volume fraction of the filler for POM/GF (⊗) and POM/GB (⊙) systems. (b) Strain energy release rate versus the volume fraction of the filler for POM/GF and POM/GB systems.

## 8. Summary

The dependence of the mechanical properties on the volume fraction of the reinforcing glass fibres and glass beads in polyoxymethylene matrix was studied. It was found that for both composite systems, the measured quantities such as tensile strength, flexural strength, flexural modulus and fracture toughness were all linear functions of the filler concentration,  $\phi$ . Consequently, it was possible to relate these quantities and use them for the prediction of mechanical properties. Also, a series of linear relationships were obtained which related the same quantity for the two reinforcing filler systems. Consequently, the mechanical properties of glass bead system could be used to determine that of the glass fibre system, and vice versa, for the same filler concentration.

Variations of impact strength and strain energy release rate with respect to filler concentration were



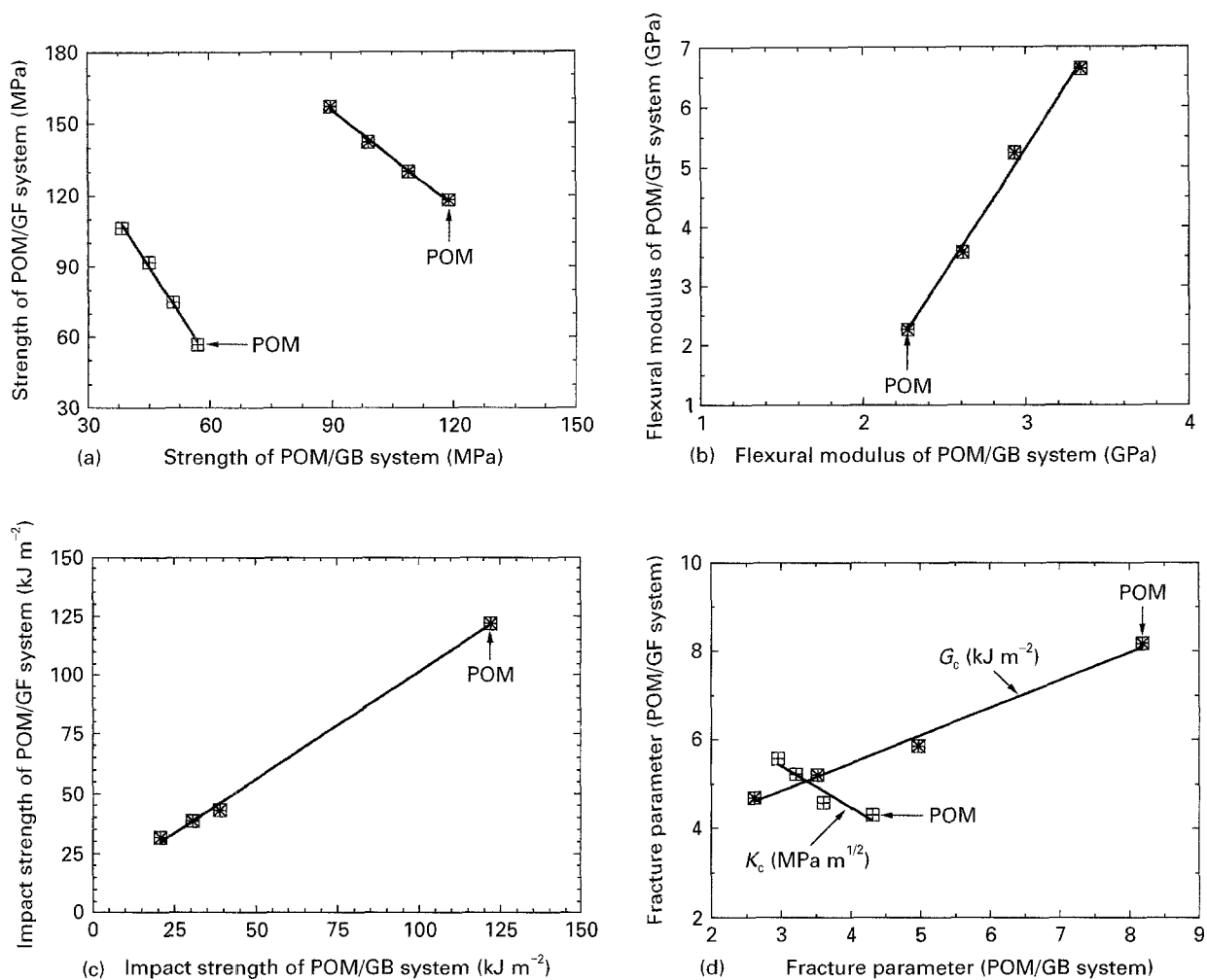


Figure 12 (a) Tensile (⊠) and flexural (⊠) strength of POM/GF system versus tensile and flexural strength of POM/GB system. (b) Flexural modulus of POM/GF system versus the flexural modulus of POM/GB system. (c) Impact strength of POM/GF system versus impact strength of POM/GB system. (d) Fracture toughness and strain energy release rate of POM/GF system versus fracture toughness and strain energy release rate of POM/GB system.

found to be non-linear for both composite systems, but the measured values for one filler system were also linearly related to that of the other system.

### Acknowledgements

The material provision by Hoechst UK is much appreciated.

### References

1. S. HASHEMI, K. J. DIN and P. LOW, *Polym. Eng. Sci.* (1996) in press.

2. W. F. BROWN and J. E. SRAWLEY, ASTM STP 410, 1966.
3. L. NICOLAIS and M. NARKIS, *Polym. Eng. Sci.* **11** (1971) 194.
4. M. R. PIGGOTT and J. LEIDNER, *J. Appl. Polym. Sci.* **18** (1974) 1619.
5. A. KELLY and W. R. TYSON, *J. Mech. Phys. of Solids.* **6** (1965) 13.
6. D. HALL, "Introduction to composite materials", Cambridge University Press, Cambridge, UK.
7. A. EINSTEIN, *Ann. der Phys.* **19**, (1906) 289.
8. R. BUCHDAHL, *J. Polym. Sci.* **28** (1958) 239.
9. N. BROWN, *Mater. Sci. Eng.* **8** (1971) 69.

Received 18 December 1995

and accepted 13 February 1996